JOURNAL of QASSIM UNIVERSITY FOR SCIENCE
© 2022 Qassim University [E-ISSN: 1658-9610]
Vol. 1, Issue 1, pp 27-41 (October 2022)

JQUS

X-Ray Diffraction Study of The Strain-Stress Thickness Profiling in GaN/Al_2O_3 Heterostructure

A. Bchetnia[1*], Asma Aedh S Almutairi[3], Fedia Ghaleb al harbi[2], Fatma Hfaiedh Esaahli[1]

[1] Department of Physics, College of Science, Qassim University, Saudi Arabia
[2] Department of Physics, College of science and arts at Alnabhania, Qassim University, Saudi Arabia
[3]Department of Physics, College of Science and Arts in Al-Rass, Qassim University, Saudi Arabia

[*]Corresponding author: O.Bchetnia@edu.qu.sa

Abstract

Gallium nitride (GaN) films were grown on c-plane sapphire substrates treated with silicon nitride (SiN) by metalorganic chemical vapor deposition. Growth started with nitridation of the substrate of the sapphire, followed by treatment with SiN and then the growth was interrupted at the different stages of the film coalescence. For the different thicknesses, the GaN microstructure state was studied by High-resolution X-ray Diffraction measurements. The a and c lattice constants were measured using symmetric and asymmetric ($\omega/2\theta$) diffraction spectra. The in-plane and out-of-plane strains were determined and compared to fully relaxed GaN film**.** As the thickness of the GaN layer increases, the compressive room temperature strain increases and remain constant when the 2D growth mode is achieved. Then, thermal, hydrostatic, and intrinsic stress levels have been determined for the different film coalescence levels. The growth of GaN layers is accompanied by intrinsic tensile stress generation which is reduced significantly with thickness and remains constant when the film reaches the 2D growth mode. The results demonstrate that all samples exhibit a lower isotopic hydrostatic

compression deformation. It is supposed that the hydrostatic strain in the epilayers is caused by native point defects. The type and concentration of the native defects suspected in the grown GaN thin films have been identified and estimated.

Keywords: HRXRD; Native defects; Stress; GaN.

I. Introduction

One of the major difficulties in the growth of III-V nitrides is the lack of adequate substrates having matched lattice parameters and accommodated thermal expansion coefficients. All nitride-based components are therefore produced by heteroepitaxy using substrates such as sapphire, SiC or Si. The strong mismatch between the substrate and the epitaxial layer creates stresses which will relax by introducing a large number of dislocations typically reaching the order of $10^{10}cm^{-2}$ [1-3]. Many studies have been devoted to understanding the structure of these defects and their formation mechanisms as well as their influence on the optoelectronic properties of nitrides [4-9].

The crystalline quality of epitaxial layers for devices based on GaN and its alloys is a crucial point in the manufacture of optoelectronic devices. Optimization of GaN growth is a very complex process. This is due to the considerable number of parameters involved at high temperatures. Among the most studied parameters we can cite: the growth temperature, the purity of the precursors, the carrier gas, the pressure, the nature of the buffer layer and the choice of the substrate, etc. [4, 10]. The performance of the electronic device is very sensitive to the microstructure of materials. Dislocations prove to be detrimental to the performance of optoelectronic devices because they constitute non-radiative recombination centers. The structure of GaN seems to be improved by using patterned substrates, ELO (Epitaxial Lateral Overgrowth) lateral growth, so-called "pendeoepitaxy" (PE) techniques, lateral growth on trenches (LOFT: Lateral Overgrowth From Trenches) or the growth on etched substrates (CE: Cantilever Epitaxy) [11, 12]. All these techniques are based on the lateral growth and the coalescence of the epitaxial layers to finally form a continuous layer. The use of these growth techniques makes it possible to reduce the high density of dislocations but does not completely solve the problem of stresses. However, experimentally, these techniques remain complicated and very expensive. In our team, we opted for the technique using the SiN treatment of the sapphire substrate. This process is done in situ and it is easy to set up and inexpensive [13]. In

situ monitoring by laser reflectometry shows that the epitaxy begins with a 3D phase on the zones which have not been masked by SiN. A phase of coalescence of the islands above the SiN pseudo-mask is accomplished through faster lateral growth and ends in a 2D phase. We have noticed that few works have studied the effect of thickness variation on the structural, electrical and optical properties of GaN epitaxially grown by the conventional (2D) growth process or by the new process known as SiN treatment (3D, coalescence and 2D).

In this paper, we report on the evolution of the strain-stress state of the GaN films versus thickness. The different contributions in the stress, thermal, hydrostatic, and intrinsic were determined and discussed.

II. Experimental

The growth of the investigated sample series was performed in a metal-organic chemical vapor deposition MOCVD vertical reactor. Two in situ sapphire preparations are investigated. The first in situ preparation is the standard nitridation performed at 1080°C, for 10 minutes under NH_3+H_2+N_2 atmosphere. The second preparation consists in the former nitridation followed by an in-situ deposition of a thin SiN mask on the sapphire. The SiN coating is obtained by introducing silane (SiH_4) in the vapor phase at the end of the nitridation step of sapphire. The GaN buffer layer with thickness of 30 nm was then deposited at 600°C. The GaN epilayer was grown at 1120°C. Details of the growth procedure can be found elsewhere [14]. The only difference between the investigated samples in this study is the thicknesses (0.12 µm (A), 0.80 µm (B), 2.00 µm (C), 4.50 µm (D)). These thicknesses were chosen since they cover all the different stages of film coalescence under the used growth conditions. Samples A and B presented partially coalesced layers. However, the GaN layers C and D have completely coalesced morphology.

HRXRD was performed using a BedeMetrix™ -L X-ray tool fitted with a Microsource™ micro-focus source, a ScribeView™ optic and a channel-cut beam conditioning crystal. The beam diameter at the sample position was less than 100 µm giving footprints of ~ 200 µm x 100 µm for the symmetric reflection and ~ 100 µm x 100 µm for the asymmetric reflection. The detector slits were set at 100 µm, giving an acceptance angle of ~50 arcsecs. The angular positions of the sample and detector were adjusted with a high precision angular position of 0.0002 deg. X-ray measurements were performed with a high-resolution diffractometer

equipped with a fourfold Ge (2 2 0) monochromator, delivering a pure CuKα1 line of wavelength (λ=0.154 nm).

III. Results and discussions

The high-resolution X-ray diffraction (HRXRD) spectra of the thickest GaN sample (D) film were measured in symmetric and asymmetric scan mode as shown in Figures 1 A and B respectively. All crystallographic structures of the as-deposited GaN samples belong to the hexagonal space group. The c-axis of GaN is textured about the [00.1] direction on a (00.1) sapphire substrate, which gives the samples wurtzite GaN characteristic peaks because of the (00.2), (00.4), and (00.6) diffractions. In the asymmetric scan mode (Figure 1 B), the reflections (10.2) and (20.4) were detected.

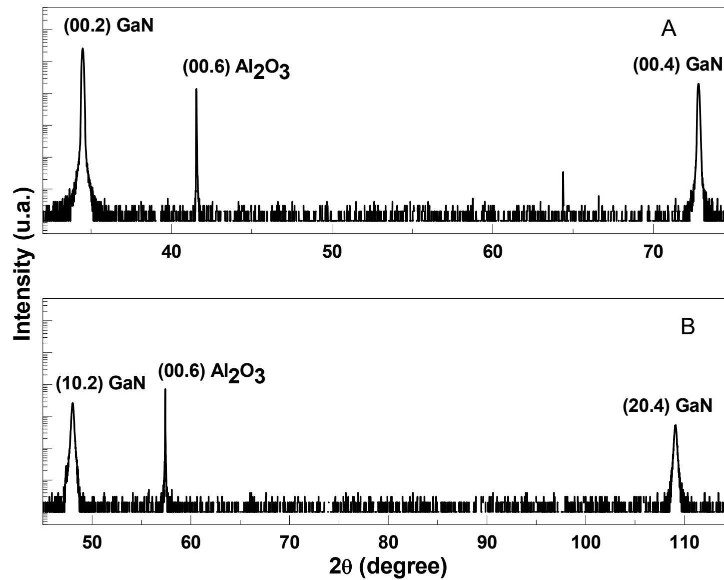

Figure 1: HRXRD w-2θ symmetric (A) and asymmetric (B) spectra from GaN/Al_2O_3 heteroepitaxial structure.

First , on the basis on Bragg's law, we determined the values of lattice parameter c from the high-angle symmetry reflection [15]. The following equation combines the lattice parameters c and a with the interplanar spacing value of hexagonal systems:

$$\frac{1}{d_{hkl}^2} = \frac{4}{3}\frac{h^2+k^2+hk}{a^2} + \frac{l^2}{c^2} \quad (1)$$

Thus, the lattice parameters a were calculated using asymmetric reflection and the estimation of c found beforehand. The founded lattice parameters variations with thickness are shown in figure 2.

To determine the relaxation level of our samples, we used the lattice parameters of fully relaxed (bulk) GaN ($a_0 = 3.1892$ Å, $c_0 = 5.1850$ Å) [16]. For the sample with the lower thickness (sample A), the lattice parameters are so close to that of the relaxed material. As the thickness increases, the layers exhibit compression in the (00.1) growth plane. The in-plane (ε_a, ε_b) and out-of-plane (ε_c) strains are determined from the relationships:

$$\begin{cases} \varepsilon_a = \varepsilon_b = \dfrac{a - a_0}{a_0} \\ \varepsilon_c = \dfrac{c - c_0}{c_0} \end{cases}$$

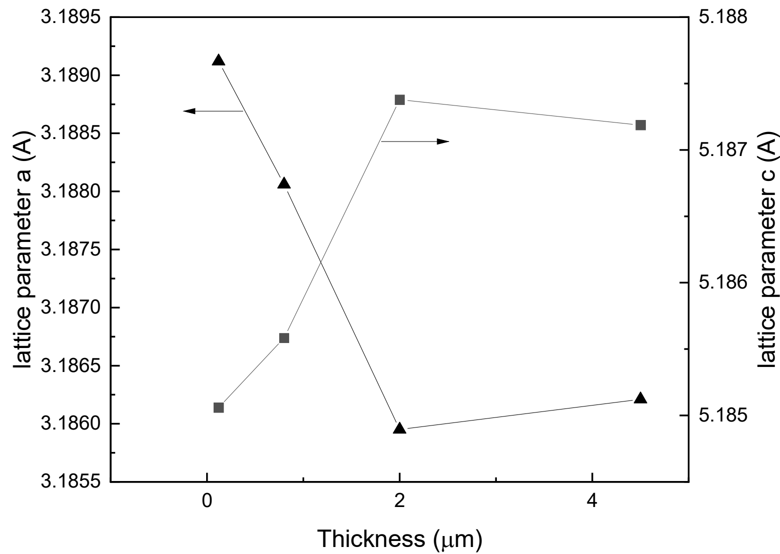

Figure 2: Lattice parameters a and c as function of thickness.

The presence of native defects and the incorporation of residual impurities cause hydrostatic deformation in GaN layer. The deformations ε_a and ε_c cohabit with the hydrostatic strain ε_h. The different types of strains are described by the following relations [17]:

$$\varepsilon_c = \varepsilon_c^b + \varepsilon_c^h \quad (2)$$

$$\varepsilon_a = \varepsilon_a^b + \varepsilon_a^h \quad (3)$$

$$\frac{\varepsilon_c^b}{\varepsilon_a^b} = -2\frac{C_{13}}{C_{33}} \quad (4)$$

$$\frac{\varepsilon_c^h}{\varepsilon_a^h} = \frac{C_{11} + C_{12} - 2C_{13}}{C_{33} - C_{13}} \quad (5)$$

where ε_c^b and ε_a^b are the pure biaxial deformations. In addition, ε_c^h and ε_a^h are the hydrostatic deformations out and in the growth plane (00.1), respectively. The used elastic constants of wurtzite GaN were C_{11} = 390 GPa, C_{12} =145 GPa, C_{13}=106 GPa and C_{33}= 398 GPa [18].

The overall hydrostatic deformation is given by:

$$\varepsilon_h = \frac{1}{3}(2\varepsilon_a^h + \varepsilon_c^h) \quad (6)$$

From the aforementioned relations, we calculated the components of the pure biaxial $(\varepsilon_a^b, \varepsilon_c^b)$ and hydrostatic $(\varepsilon_a^h, \varepsilon_c^h)$ deformations. The representative obtained values are plotted in figure 3.

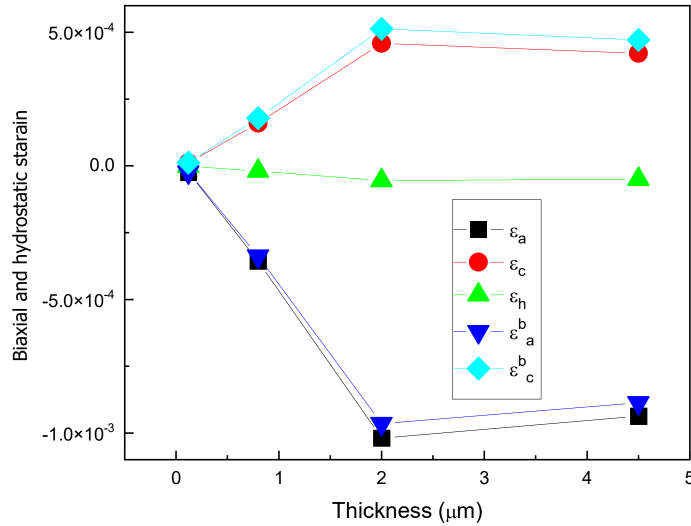

Figure 3: Hydrostatic ε_h , in and out of the growth plane pure biaxial deformations (ε_c^b , ε_a^b) and the in-plane (ε_a) and out-of-plane (ε_c) total strains as function of thickness.

The hydrostatic deformation is in compression with small amount compared to the biaxial deformation. We founded a small gap between ε_a^h and ε_c^h indicating the isotropy of hydrostatic deformation. In general, the hydrostatic deformation is caused by native defects. The interstitials (Ga_i, N_i) as well as the nitrogen anti-sites (N_{Ga}), cause an extension of the crystal lattice. In our case, for the different coalescence degree, the hydrostatic strain is in compression. The relative concentration of defects, such as anti-sites (Ga_N) and vacancies (V_{Ga}, V_N), would be more dominant. Gallium and nitrogen vacancies introduce acceptor and donor states, respectively. MOCVD GaN grown layers were n-type and prepared with a high V/III ratio. It is therefore probable that the concentration of nitrogen vacancies is greater than that of gallium vacancies and Ga_N anti-sites. Table 1 shows the formation energies of the main native defects that could be present in the GaN layers [19]. The formation energy of the Ga_N and N_{Ga} anti-sites is extremely high, which makes their formation doubtful. On the other hand, the formation energy of the nitrogen vacancy V_N is lower than that of the Ga vacancies (V_{Ga}). This suggests that the first type of native defect (V_N) remains one of the main faults in GaN.

Table 1: Formation energy of native defects in GaN [19].

Defaults	Formation energy (eV)
V_N	4.6
V_{Ga}	6.3
N_{Ga}	5.8
Ga_N	10.5
O_N	0.7

Several studies[20, 1] have reported that nitrogen vacancies and oxygen at the nitrogen sites are responsible for the n-type residual doping of GaN. Because the oxygen atomic radius is slightly lower than that of nitrogen, oxygen causes a low hydrostatic tension that is almost negligible compared with the effect of nitrogen vacancies[18]. We attribute the hydrostatic deformation to the set of defects (O_N and V_N) and the effect of the conduction electrons. The following relationship was proposed for the different components of hydrostatic deformation [14]:

$$\varepsilon_h = \beta_V N_V + \beta_o N_o + \beta_e n \tag{7}$$

The concentration of nitrogen vacancies is given by the relation:

$$N_V = \frac{\varepsilon_h - \beta_o N_o - \beta_e n}{\beta_V} \tag{8}$$

With $\beta_V = -\frac{1}{N_s}$ (9)

$$\beta_o = \frac{1}{3}\left[1 - \left(\frac{r_o}{r_N}\right)^3\right] N_s^{-1} \tag{10}$$

$$\beta_e = -\frac{a_c}{3B} \tag{11}$$

The different parameters used to calculate the concentration of nitrogen vacancies are recorded in table 2 [19].

Table 2: Characteristic parameters of hydrostatic deformation. N_s is the atomic density of GaN; r_O and r_N are the atomic rays of oxygen and nitrogen, respectively; B is the elastic modulus of the GaN and a_c is the energy deformation potential of the conduction band [19].

r_o (nm)	r_N (nm)	a_c (eV)	B (GPa)	β_V (cm^{-3})	β_O (cm^{-3})	β_h (cm^{-3})
0.0678	0.0719	-2.8	202	1.136×10^{-23}	-4.737×10^{-23}	1.25×10^{-24}

Table 3 shows the concentration of free electrons (n) measured by the Hall effect (not presented here), the number of oxygen atoms (N_O) measured by SIMS, and the calculated density of nitrogen vacancies (N_V).

Table 3: concentrations of oxygen (N_O), free electrons (n), and nitrogen vacancies (N_v).

Sample	n ($cm^{-3}\times 10^{17}$)	$N_0\times 10^{17}$(cm^{-3})	$N_V\times 10^{17}$(cm^{-3})
A	251.7	5.1	7.6
B	76.6	5.1	4.7
C	36.2	4.6	35.0
D	2.3	3.9	30.0

The hydrostatic stress is given by the following relation:

$$\sigma_h = M \times \varepsilon_h \qquad (12)$$

where M= 449.6 GPa is the Young modulus, σ_h is the hydrostatic stress and ε_h is the hydrostatic strain.

This compressive stress is relatively low compared with the biaxial stress. It reaches a maximum value of approximately -2.5×10^{-2} GPa for the layers C and D. Harutyunyan et al.[18] measured the hydrostatic stress for different V/III ratios of the buffer layer and found a minimum value of the order of -1.5×10^{-1} GPa. A value of -7×10^{-2} GPa has been found in GaN layers doped with Si[21]. The reduction in the hydrostatic component is directly related to a decrease in the concentration of native defects in the GaN layers treated with SiN. Therefore, this can help to limit the harmful effects of these defects (compensation, non-radiative recombination centres, etc.).

At the end of growth, and during cooling, the mismatch between the coefficients of thermal expansion of GaN (α_{GaN}) and sapphire (α_{saphir}) generates a deformation of the lattice parameters in the growth plane. The GaN layers will therefore be in biaxial compression. The thermal deformation is given by the following expression:

$$\varepsilon_{th} = \int_{Tc}^{Ta} \Delta\alpha \times dT \quad (13)$$

where Tc and Ta represent the growth and the ambient temperature respectively, $\Delta\alpha$ is the difference between the thermal expansion coefficients of GaN and sapphire substrate. The dependence of $\Delta\alpha$ on temperature has often been neglected [22]. This leads to the simple expression:

$$\varepsilon_{th} = \Delta\alpha \times \Delta T \quad (14)$$

ΔT is the difference between the growth temperature (1393°K) and the ambient temperature (300°K).

The ε_{th} value found is of the order of -3.5 $x10^{-3}$. Wareil et al. [23] proposed a theoretical calculation model of the thermal deformation. Taking into account the variation of $\Delta\alpha$ as a function of temperature. They founded a value of -2 $x10^{-3}$. This is in good agreement with the experimental results found in references [22, 24]. In our calculation that follow, we adopt the value of -2 $x10^{-3}$, which seems to be more rigorous. The dispersion of the values of the thermal deformation is probably due to the great diversity of the values of the coefficients of thermal expansion present in the literature [25, 26].

The following relationship translates the link between thermal stress and the deformation it causes: $\sigma_{th} = M \times \varepsilon_{th}$ (15)

where M = 449.6 GPa is the biaxial modulus given by the elastic coefficients and ε_{th} is the thermal strain.

The calculated value is -0.9 GPa. This is in good agreement with that determined by Hearne et al. [27] by monitoring the curvature of the layer. They used ex-situ X-ray diffraction measurements for the determination of the biaxial strain. The thermal stress is calculated by a simple subtraction of the values found in situ and ex situ.

The relatively high value of the biaxial strain implies the presence of significant residual stresses that come from the layer/substrate interface. The intrinsic stress in tension is determined by subtracting from the biaxial stress, the thermal and hydrostatic components [22].

$$\sigma_{int} = \sigma_a - \sigma_h - \sigma_{th} \quad (16)$$

In figure 4, we resumed all the stresses types amount involved in the GaN/Al_2O_3 structure as function of thickness. We noted that before the coalescence (layers A and B), the intrinsic tensile stress is reduced significantly with thickness. But when coalescence is reached, the tensile stress is almost constant (layers C and D). Our results are in agreement with those presented in references [22, 28], showing that this intrinsic tensile stress depends on the state of coalescence of the layers.

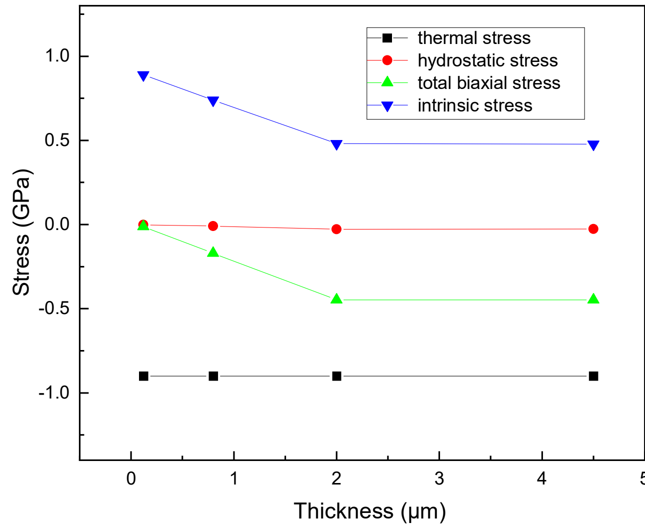

Figure 4: Values of the different components of stress (total, thermal, hydrostatic and intrinsic component) as a function of thickness.

IV. Conclusion

We developed a series of GaN layers with different thicknesses. The different growth stages of GaN on a SiN-treated sapphire substrate (00.1) are present in the selected thickness range (0.1 to 4 µm). The layers were characterised utilizing HRXRD. The lattice parameters a and c of the GaN layers were determined. We have extracted the values of the pure bi-axial strain in and out of the growth plane. The obtained values showed a good isotropic structural property. At room temperature, the layers were subjected to biaxial compression. By comparison to GaN

layers grown without SiN treatment, our samples exhibited a lower stress value. The thermal, hydrostatic and intrinsic components of the stress were determined. We associated the hydrostatic compression strain to the presence of nitrogen vacancies and oxygen at the nitrogen sites. The concentration of the native defects responsible for hydrostatic deformation was determined. The compressive stress of the GaN layers increased with thickness and remained constant in the 2D growth phase.

References

[1] A. F. Wright and Ulrike Grossner. The effect of doping and growth stoichiometry on the core structure of a threading edge dislocation in GaN**.** Appl. Phys. Lett (1998), 73, pp 2751. https://doi.org/10.1063/1.122579.

[2] Vladimir Lucian Ene, Doru DINESCU, Iulia ZAI, *et al.* Study of Edge and Screw Dislocation Density in GaN/Al2O3 Heterostructure. *Materials* (2019), vol. 12, no 24, p. 4205.

https://doi.org/10.3390/ma12244205

[3] Hiroyuki Shinoda and Nobuki Mutsukura. "Structural properties of GaN layers grown on Al2O3 (0001) and GaN/Al2O3 template by reactive radio-frequency magnetron sputter epitaxy." *Vacuum* 125 (2016): 133-140.

https://doi.org/10.1016/j.vacuum.2015.12.008

[4] U. Rossow, F. Hitzel, N. Riedel, S. Lahmann, J. Bläsing, A. Krost, ... & A. Hangleiter. A. Influence of low-temperature interlayers on strain and defect density of epitaxial GaN layers. *Journal of crystal growth* (2003), *248*, 528-532.

https://doi.org/10.1016/S0022-0248(02)01883-3

[5] M. Vorobiov, O. Andrieiev, D. O. Demchenko, & M. A. Reshchikov. Point defects in beryllium-doped GaN. *Physical Review B* (2021), *104*(24), 245203.

https://doi.org/10.1103/PhysRevB.104.245203

[6] M. Grabowski, E. Grzanka, S. Grzanka, *et al.* The impact of point defects in n-type GaN layers on thermal decomposition of InGaN/GaN QWs. *Sci Rep* **11** (2021)**,** 2458. https://doi.org/10.1038/s41598-021-81017-w

[7] T. J. Ruggles, J. I. Deitz, A. A. Allerman, C. B. Carter, & J. R. Michael. Identification of star defects in gallium nitride with HREBSD and ECCI. *Microscopy and Microanalysis* (2021), *27*(2), 257-265.

https://doi.org/10.1017/S143192762100009X

[8] F. Wang, R. Zhang, D.Q. Lu, X.Q. Xiu, S.L. Gu, B. Shen, Y. Shi, Y.D. Ye, Y.D. Zheng. Investigation of the crystal tilts in laterally epitaxial overgrowth GaN films formed by hydride vapor phase epitaxy. *Optical Materials* (2003), *23*(1-2), 123-126.

https://doi.org/10.1016/S0925-3467(03)00072-7

[9] N. Gmeinwieser, P. Gottfriedsen, U.T. Schwarz, W. Wegscheider, R. Clos, A. Krtschil, A. Krost, K. Engl, A. Weimar, G. Bruderl, A. Lell, V. Harle. Long range strain and electrical potential induced by single edge dislocations in GaN. *Physica B: Condensed Matter* (2006), *376*, 451-454.

https://doi.org/10.1016/j.physb.2005.12.116

[10] R. chierhia, T. Böttcher, H Heinke, S. Eonfeldt, S. Figge, D. Hommel. Microstructure of heteroepitaxial GaN revealed by x-ray diffraction. *Journal of Applied physics* (2003), *93*(11), 8918-8925.

https://doi.org/10.1063/1.1571217

[11] A. Krost, A. Dadgar, F. Schulze, J. Blasing, G. Strassburger, R. Clos, A. Diez, P. Veit, T. Hempel, J. Christen. In situ monitoring of the stress evolution in growing group-III-nitride layers. *Journal of crystal growth* (2005), *275*(1-2), 209-216.

https://doi.org/10.1016/j.jcrysgro.2004.10.090.

[12] K. Pakuła, R. Bożek, J. M. Baranowski, J. Jasinski, Z. Liliental Weber. Reduction of dislocation density in heteroepitaxial GaN: role of SiH4 treatment. *Journal of crystal growth* (2004), *267*(1-2), 1-7.

https://doi.org/10.1016/j.jcrysgro.2004.03.020.

[13] I. Halidou, Z. Benzarti, T. Boufaden, B. El Jani, S. Juillaguet, M. Ramonda. Influence of silane flow on MOVPE grown GaN on sapphire substrate by an in situ SiN treatment. Materials Science and Engineering: B. (2004), 110(3), 251-255. https://doi.org/10.1016/j.mseb.2004.02.002.

[14] A. Bchetnia, T. A. Lafford, Z. Benzarti, I. Halidou, M. M. Habchi, B. El Jani. Effect of thickness on structural and electrical properties of GaN films grown on SiN-treated sapphire. *Journal of crystal growth* (2007), *308*(2), 283-289.

https://doi.org/10.1016/j.jcrysgro.2007.09.006.

[15] M. A. Moram, M. E. Vickers. X-ray diffraction of III-nitrides. *Reports on progress in physics*, 2009, vol. 72, no 3, p. 036502.

https://iopscience.iop.org/article/10.1088/0034-4885/72/3/036502/meta

[16] H. Lahrèche, M. Leroux, M. Laugt, M. Vaille, B. Beaumont, P. Gibart. Buffer free direct growth of GaN on 6H–SiC by metalorganic vapor phase epitaxy. *Journal of Applied Physics* (2000), *87*(1), 577-583.

https://doi.org/10.1063/1.371902

[17] L. B. Freund, Eric Chason. Model for stress generated upon contact of neighboring islands on the surface of a substrate. Journal of Applied Physics 89.9 (2001): 4866-4873.

https://doi.org/10.1063/1.1359437

[18] V. S. Harutyunyan, P. Specht, J. Ho, E. R Weber. Anisotropy of the elastic properties of wurtzite InN epitaxial films. In *Defect and Diffusion Forum* ((2004), Vol. 226, pp. 79-90). Trans Tech Publications Ltd.

https://doi.org/10.4028/www.scientific.net/DDF.226-228.79

[19] V. S. Harutyunyan, A. P. Aivazyan, E. R. Weber, Y. Kim, Y. Park and S. G. Subramanya. High-resolution x-ray diffraction strain-stress analysis of GaN/sapphire heterostructures. *Journal of Physics D: Applied Physics* (2001), *34*(10A), A35.

https://iopscience.iop.org/article/10.1088/0022-3727/34/10A/308/meta

[20] D.C Look and J. R Sizelove. Dislocation scattering in GaN. *Physical review letters* (1999), *82*(6), 1237.

https://doi.org/10.1103/PhysRevLett.79.2273

[21] C. Kisielowski, J. Kruger, S. Ruvimov, T. Suski, J. W. Ager III, Jones, Z. Lilienal-Weber, M. Rubin, and E. R. Weber and M. D. Bremser, R. F. Davis. Strain-related phenomena in GaN thin films. *Physical review B* (1996), *54*(24), 17745.

https://doi.org/10.1103/PhysRevB.54.17745

[22] T. Bottcher, S. Einfeldt, S. Figge, R. Chierchia, H. Heinke, D. Hommel, J. S. Speck. The role of high-temperature island coalescence in the development of stresses in GaN films. *Applied Physics Letters* (2001), *78*(14), 1976-1978.

https://doi.org/10.1063/1.1359780

[23] Waeil M. Ashmaw, Mohamed A. Zikry, Kai wang, Robert R. Reeber. Modeling of residual stresses for thermally strained GaN/Al2O3 heterostructures. *Journal of crystal growth* (2004), *266*(4), 415-422.

https://doi.org/10.1016/j.jcrysgro.2004.02.105

[24] A. Cremades, L. Görgens, O. Ambacher, M. Stutzmann, F. Scolz. Structural and optical properties of Si-doped GaN. *Physical Review B*, 2000, vol. 61, no 4, p. 2812.

https://doi.org/10.1103/PhysRevB.61.2812

[25] Sukit Limpijumnong and G. Chris Van de Walle. "Diffusivity of native defects in GaN." *Physical Review B* 69.3 (2004): 035207.

https://doi.org/10.1103/PhysRevB.69.035207

[26] M. Leszczynski, H. Teisseyre, T. Suski, I. Grzegory, M. Bockowski, J. Jun, J., ... & T. S. Cheng, Lattice parameters of gallium nitride. *Applied Physics Letters* (1996), *69*(1), 73-75.

https://doi.org/10.1063/1.118123

[27] S. Hearne, E. Chason, J. Han, J. A. Floro, J. Figiel, J.Hunter, H. Amano, I. S. T. Tsong Stress evolution during metalorganic chemical vapor deposition of GaN. *Applied Physics Letters* (1999), *74*(3), 356-358.

https://doi.org/10.1063/1.123070

[28] J. Napierala, D. Martin, N. Grandjean, M. Ilegems. Stress control in GaN/sapphire templates for the fabrication of crack-free thick layers. *Journal of crystal growth* (2006), *289*(2), 445-449.

https://doi.org/10.1063/1.2213175